



Crown Glass Drilling by Short-Pulse CO₂ Laser with Tunable Pulse Tail

Md. Ekhlalur Rahaman¹ · Kazuyuki Uno¹

Accepted: 10 January 2022 / Published online: 22 January 2022

© The Author(s), under exclusive licence to Springer Science+Business Media, LLC, part of Springer Nature 2022

Abstract

Hole drilling in crown glass with a large thermal expansion coefficient of 94×10^{-7} /K by a longitudinally excited short-pulse CO₂ laser with a tunable laser pulse tail was investigated. The CO₂ laser produced short laser pulses with a pulse width of about 250 ns, a pulse tail with a length of 31.4 to 134.7 μ s, a spike pulse to pulse tail energy ratio of 1:7 to 1:92, and a fluence per single pulse of 6.0 to 37.9 J/cm² at a repetition rate of 1 to 400 Hz. Sample cooling was not employed in the drilling process. At a repetition rate of 1 to 90 Hz, the CO₂ laser pulses produced cracks. At a repetition rate of 100 to 140 Hz, the CO₂ laser pulses occasionally produced cracks and crack-free holes. At a repetition rate of 150 to 400 Hz, the CO₂ laser pulses produced crack-free holes. Under various irradiation conditions, the hole depth and estimated hole volume per total irradiation fluence depended on the fluence per single pulse but did not depend on the laser pulse waveform or repetition rate.

Keywords Pulsed CO₂ laser · Glass drilling · Crown glass · Laser pulse waveform · Laser fluence

Introduction

Micromachining processes such as drilling, cutting, or grooving on transparent and non-transparent materials are required in the fields of optoelectronics, sensing, aerospace engineering, etc. [1–12]. Various micromachining techniques, including mechanical, chemical, and thermal (laser-based) systems, are being developed to make the process simpler and improve processing accuracy, but they are still limited in terms of the types and geometry of materials that can be processed [5]. Among

✉ Md. Ekhlalur Rahaman
j19dtsa1@yamanashi.ac.jp; ekhlaseceku@gmail.com

¹ Integrated Graduate School of Medicine, Engineering, and Agricultural Sciences, University of Yamanashi, 4-3-11 Takeda, Kofu, Yamanashi 400-8511, Japan

the various systems for drilling glass substrates, laser-based drilling systems have been showing improved drilling quality over the past decade.

Gas lasers, especially CO₂ lasers, have become popular due to their numerous benefits, including accurate processing, low cost, easy maintenance, and efficient absorption of CO₂ laser wavelengths in glass materials. CO₂ lasers emitting at mid-infrared wavelengths of 9.2–11.4 μm (mainly 9.6 and 10.6 μm) can produce continuous wave (CW) laser light, a long laser pulse with a pulse width of 10 μs to 10 ms, a short laser pulse with a spike pulse width of 10 ns to 1 μs and a pulse tail length of several microseconds to several tens of microseconds, or a tail-free short laser pulse with a pulse width of about 10 ns to 1 μs [13–17].

In CO₂ laser processing, a short-pulse CO₂ laser gives less thermal damage like melting, debris formation, micro-cracks, etc. than a long-pulse CO₂ laser [18–20]. The thermal damage depends on the parameters of the radiated laser light, such as the pulse width and the repetition rate, and the sample conditions, such as the thermal expansion coefficient, the thermal diffusivity, and the thermal conductivity [21, 22]. In glass processing using short-pulse CO₂ lasers, a TEA-CO₂ laser with a high spike pulse and a small pulse tail produced crack-free holes in various glasses, such as silica glass with a thermal expansion coefficient of 5.5×10^{-7} /K [23], alkali-free glass with a thermal expansion coefficient of 32×10^{-7} /K [24], and soda-lime glass with a thermal expansion coefficient of 87×10^{-7} /K [25]. The thermal expansion coefficient is one of the considerable parameters of glass processing. In laser processing of glass, glass with a higher thermal expansion coefficient has a higher tendency of producing crack than a glass with a lower thermal expansion coefficient. In this study, drilling of crown glass with a large thermal expansion coefficient of 94×10^{-7} /K by a short-pulse CO₂ laser with a tunable pulse tail was investigated. Our CO₂ laser had a spike pulse width of about 250 ns, a pulse tail length of 31.4 to 134.7 μs, spike pulse to pulse tail energy ratios of 1:7 to 1:92, and a fluence per single pulse of 6.0 to 37.9 J/cm² at a repetition rate of 1 to 400 Hz. Sample cooling was not employed in the drilling process. Laser pulses at a repetition rate of 150 to 400 Hz produced crack-free holes.

Experimental Setup

Figure 1 shows a schematic diagram of the processing system using a longitudinally excited CO₂ laser system [14, 17]. The mirror and the output coupler were selected for the wavelength of 10.6 μm, and the operating wavelength of the CO₂ laser was 10.6 μm.

Figure 2 shows an example of laser pulse waveforms. The laser pulse waveforms were measured by a photon drag detector (Hamamatsu Photonics, B749). In this study, the laser pulse waveform was controllable at a repetition rate of 1 to 400 Hz. The spike pulse width was about 250 ns at the full width half maximum (FWHM) of the spike pulse. The pulse tail length, defined as the length from the end of the spike pulse to the end of the pulse tail, was 31.4 to 134.7 μs. The energy ratio of the spike pulse to the pulse tail was 1:7 to 1:92. The laser beam was circular with a beam quality factor, M^2 , of 3.1 to 7.9 and a beam diameter of about 11.5 to 13.5 mm. A

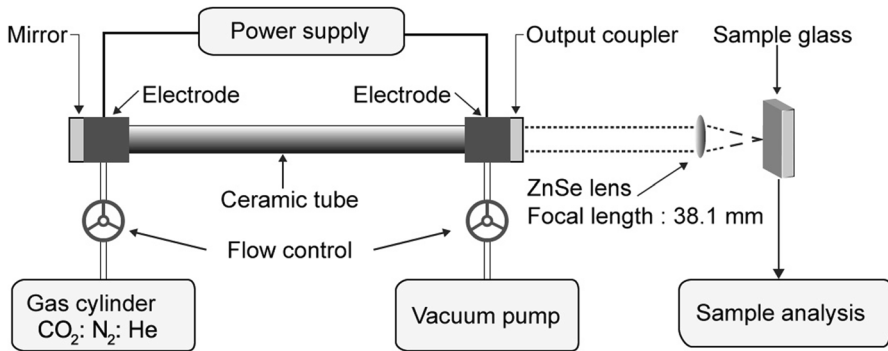


Fig. 1 Schematic diagram of a laser processing system using a longitudinally excited CO₂ laser

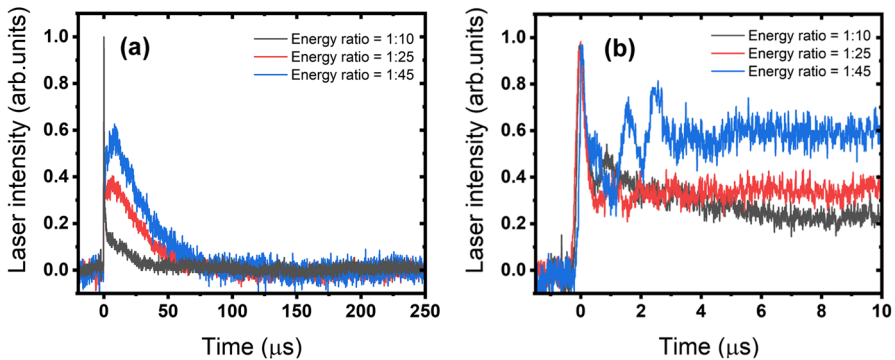


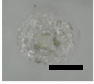

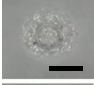
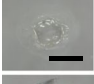
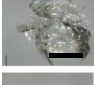


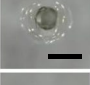
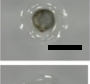
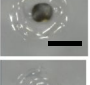
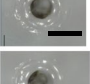
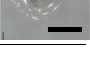
Fig. 2 Example of laser pulse waveforms at a repetition rate of 200 Hz. Laser intensity was normalized to the maximum value of the spike pulse. Black, red, and blue lines represent laser pulse waveforms with energy ratios of 1:10, 1:25, and 1:45 respectively. (a) Overall waveform. (b) The magnified timescale of spike pulse

ZnSe focusing lens was used with a focal length of 38.1 mm to focus the laser beam onto the sample surface. The numerical aperture (NA) was 0.151 to 0.176, and the depth of focus (DOF) was 231.5 to 291.9 μm . The focus spot diameter was 236.4 to 309.4 μm . A percussion laser drilling process was used in which multiple laser pulses were radiated on the sample. The sample was a crown glass slide (Matsunami, S1127) with a thermal expansion coefficient of $94 \times 10^{-7} / \text{K}$ and a thickness of 1150 μm .

Results and Discussion

Firstly, to investigate the required laser parameters that will produce crack-free holes in crown glass, 50 laser pulses with an energy ratio of 1:7 to 1:92 and a fluence per single pulse of 6.0 to 37.9 J/cm^2 were radiated on the sample surface at a repetition

Table 1 Presence and absence of cracks in the crown glass depending on the CO₂ laser parameters. The length of the scale bar is 200 μm in all images

Rept. rate (Hz)	Energy ratio	Fluence/pulse (J/cm ²)	Beam Quality: M ²	Avg. Spot diameter (μm)	Avg. NA	No. of pulses	Crack or Crack-free	Image of a hole with crack	Image of a crack-free hole
1	1:14–1:40	6.2–14.0	4.5–7.9	309.4	0.178	50	Crack		×
10	1:12–1:57	6.0–17.1	4.9–7.1	288.6	0.171	50	Crack		×
50	1:16–1:60	7.4–14.3	3.4–7.3	308.1	0.171	50	Crack		×
90	1:14–1:51	7.4–14.5	4.6–6.7	299.7	0.171	50	Crack		×
100	1:27–1:70	8.8–22.1	3.4–6.5	282.4	0.176	50	Both		
140	1:12–1:65	7.3–22.9	4.5–6.3	288.9	0.166	50	Both		
150	1:15–1:57	8.9–25.2	4.8–6.7	288.2	0.166	50	Crack-free	×	
200	1:7–1:92	10.1–37.9	4.0–5.3	236.6	0.163	50	Crack-free	×	
300	1:12–1:44	17.4–28.9	3.1–4.7	236.4	0.163	50	Crack-free	×	
400	1:9–1:18	10.7–18.4	3.5–4.7	240.1	0.163	50	Crack-free	×	

rate of 1 to 400 Hz. Table 1 shows the presence and absence of cracks in the crown glass depending on the CO₂ laser parameters. At a repetition rate of 1 to 90 Hz, laser pulses did not produce crack-free holes on the crown glass surface. At a repetition rate of 100 to 140 Hz, laser pulses produce cracks and crack-free holes. At a repetition rate of 150 to 400 Hz, crack-free holes were produced.

Figure 3 shows a top view and a side view of the sample surface irradiated by 30 pulses with an energy ratio of 1:25, a fluence per single pulse of 34.1 J/cm² and an irradiation diameter of 241.8 μm at a repetition rate of 200 Hz. The drilled hole did not have any cracks. A heat affected zone (HAZ) with a width of 114.2 μm was produced around the drilled hole. The hole diameter of the sample surface was about 122.2 μm and was 0.505 times the irradiation diameter. The hole depth was 923.4 μm, and the estimated hole volume was about 3.61 × 10⁶ μm³. The hole

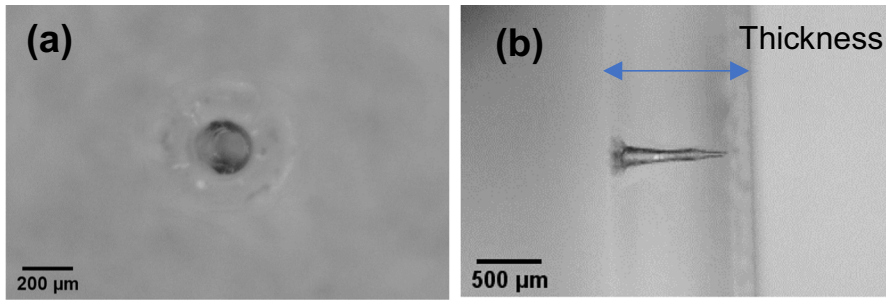


Fig. 3 Top and side views of the crown glass sample irradiated by 30 pulses with an energy ratio of 1:25 and a fluence per single pulse of 34.1 J/cm^2 at a repetition rate of 200 Hz

volume was estimated by the volume formula of a cone as the holes appeared to have conical shapes.

Figure 4 shows how the surface hole diameter, the ratio of hole diameter to irradiation diameter, the hole depth, and the estimated hole volume depended on the laser pulse waveform, the fluence per single pulse, and the total irradiation fluence, which is the product of the number of pulses and the fluence per single pulse, at

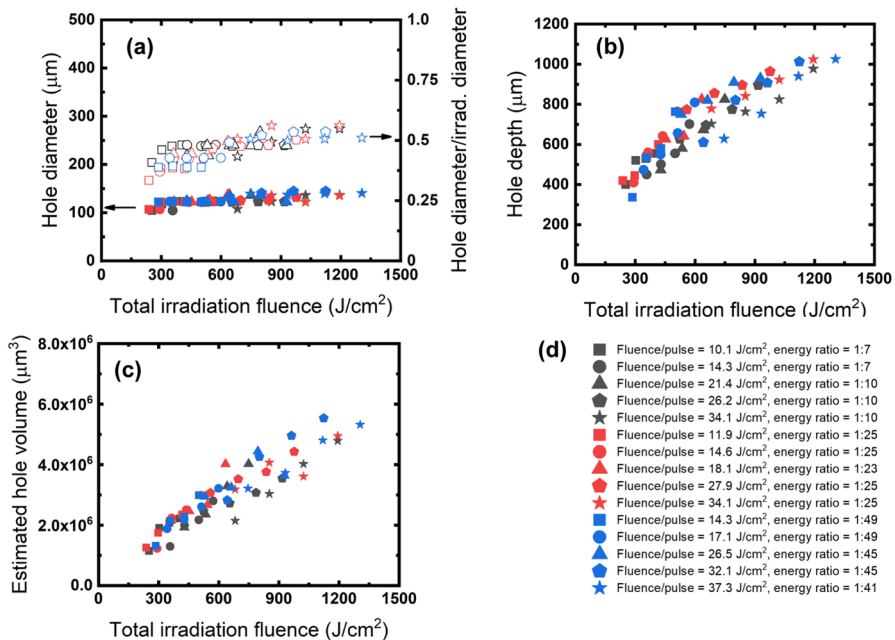


Fig. 4 Dependence of surface hole diameter, the ratio of hole diameter to irradiation diameter, hole depth, and estimated hole volume on laser pulse waveforms and total irradiation fluence at a repetition rate of 200 Hz. (a) Surface hole diameter and the ratio of hole diameter to irradiation diameter. (b) Hole depth. (c) Estimated hole volume. (d) Legend of (a), (b) and (c)

Table 2 Dependence of hole depth and estimated hole volume per total irradiation fluence on laser pulse waveforms and fluence per single pulse at a repetition rate of 200 Hz. The hole depth and estimated hole volume per total irradiation fluence are the slopes of Fig. 4(b) and (c), respectively

Symbol in Fig. 4(b), (c)	Laser pulse waveform	Fluence/pulse (J/cm^2)	Beam quality: M^2	NA	Hole depth/total irradiation fluence ($\mu m/J/cm^2$)	Estimated hole volume/total irradiation fluence ($\mu m^3/J/cm^2$)
■	1:7	10.1	4.4	0.151	1.54	5.55×10^3
●	1:7	14.3	4.4	0.151	1.19	4.37×10^3
▲	1:10	21.4	4.4	0.151	1.07	4.85×10^3
◆	1:10	26.2	4.4	0.151	1.06	4.15×10^3
★	1:10	34.1	4.4	0.151	0.89	3.66×10^3
■	1:25	11.9	4.2	0.166	1.56	5.70×10^3
●	1:25	14.6	4.2	0.166	1.48	5.48×10^3
▲	1:23	18.1	4.2	0.166	1.35	5.66×10^3
◆	1:25	27.9	4.2	0.166	1.17	4.89×10^3
★	1:25	34.1	4.1	0.166	0.99	4.33×10^3
■	1:49	14.3	5.3	0.166	1.39	5.46×10^3
●	1:49	17.1	5.3	0.166	1.37	5.27×10^3
▲	1:45	26.5	4.5	0.166	1.20	4.99×10^3
◆	1:45	32.1	4.0	0.166	0.95	4.95×10^3
★	1:41	37.3	4.2	0.166	0.82	4.16×10^3

a repetition rate of 200 Hz. Black square, circle, triangle, diamond and star symbols represent laser pulse waveforms with an energy ratio of about 1:9 and a fluence per single pulse of 10.1 J/cm^2 , 14.3 J/cm^2 , 21.4 J/cm^2 , 26.2 J/cm^2 and 34.1 J/cm^2 , respectively. Red square, circle, triangle, diamond and star symbols represent laser pulse waveforms with an energy ratio of about 1:25 and a fluence per single pulse of 11.9 J/cm^2 , 14.6 J/cm^2 , 18.1 J/cm^2 , 27.9 J/cm^2 and 34.1 J/cm^2 , respectively. Blue square, circle, triangle, diamond and star symbols represent laser pulse waveforms with an energy ratio of about 1:46 and a fluence per single pulse of 14.3 J/cm^2 , 17.1 J/cm^2 , 26.5 J/cm^2 , 32.1 J/cm^2 and 37.3 J/cm^2 , respectively. Figure 4(a) shows the dependence of a hole diameter on a total irradiation fluence. The hole diameters were almost constant throughout the total irradiation fluence, and the average hole diameter was about 125.8 μm which was about 0.46 times the irradiation diameter. Figure 4(b) and (c) shows the dependence of a hole depth and an estimated hole volume on a total irradiation fluence. The hole depth and the estimated hole volume increases with the increase of the total irradiation fluence which is a natural phenomenon and similar characteristics reported in [26, 27]. Moreover, to understand the dependence of the hole depth and the estimated hole volume per total irradiation fluence on the energy ratio of the laser pulse waveform and the fluence per single pulse, the irradiation conditions were divided into three groups depending on the energy ratios in the laser pulse waveform. The three groups of energy ratios were black symbols with the energy ratio of about 1:9, red symbols with the energy ratios of about 1:25 and blue symbols with the energy ratios of about 1:46. Table 2 is the slopes of Fig. 4(b) and (c) and shows hole depth and the estimated hole volume per total irradiation fluence decreased with the increase of the fluence per single pulse. For example, the almost same fluence per single pulse of about 14.4 J/cm^2 in the

three groups of energy ratios produced the almost same hole depth per total irradiation fluence of about $1.35 \mu\text{m}/\text{J}/\text{cm}^2$ and produced the almost same estimated hole volume per total irradiation fluence of about $5.10 \times 10^3 \mu\text{m}^3/\text{J}/\text{cm}^2$. Again, the almost same fluence per single pulse of about $26.9 \text{ J}/\text{cm}^2$ in the three groups of energy ratios produced the almost same hole depth per total irradiation fluence of about $1.14 \mu\text{m}/\text{J}/\text{cm}^2$ and produced the almost same estimated hole volume per total irradiation fluence of about $4.67 \times 10^3 \mu\text{m}^3/\text{J}/\text{cm}^2$. Similarly, the almost same fluence per single pulse of about $33.4 \text{ J}/\text{cm}^2$ in the three groups of energy ratios produced the almost same hole depth per total irradiation fluence of about $0.94 \mu\text{m}/\text{J}/\text{cm}^2$ and produced the almost same estimated hole volume per total irradiation fluence of about $4.31 \times 10^3 \mu\text{m}^3/\text{J}/\text{cm}^2$. Therefore, the hole depth and the estimated hole volume per total irradiation fluence did not depend on the energy ratio of the laser pulse waveform but depended on a fluence per single pulse. Furthermore, repetition rates of 200 Hz, 300 Hz and 400 Hz were considered to realize the dependence of the hole depth and the estimated hole volume per total irradiation fluence on the repetition rate. Table 3 shows the dependence of the drilling characteristics on the three repetition rates. The hole depth and the estimated hole volume per total irradiation fluence did not depend on the repetition rate but depended on a fluence per single pulse. For example, the almost same fluence per single pulse of about $14.1 \text{ J}/\text{cm}^2$ in three repetition rates produced the almost same hole depth per total irradiation fluence of $1.12 \mu\text{m}/\text{J}/\text{cm}^2$ and produced the almost same estimated hole volume per total irradiation fluence of about $4.40 \times 10^3 \mu\text{m}^3/\text{J}/\text{cm}^2$. Similarly, the almost same fluence per single pulse of about $18.4 \text{ J}/\text{cm}^2$ in three repetition rates produced the almost same hole depth per total irradiation fluence of $0.90 \mu\text{m}/\text{J}/\text{cm}^2$ and produced the almost

Table 3 Dependence of hole depth and estimated hole volume per total irradiation fluence of 50 pulses on repetition rate of 200 to 400 Hz

Rept. rate (Hz)	Laser pulse waveform	Fluence/pulse (J/cm^2)	Beam quality: M^2	NA	Hole depth (μm)	Hole depth/total irradiation fluence ($\mu\text{m}/\text{J}/\text{cm}^2$)	Estimated hole volume/total irradiation fluence ($\mu\text{m}^3/\text{J}/\text{cm}^2$)
200	1:25	14.2	4.4	0.151	777.9	1.09	4.32×10^3
200	1:40	16.4	4.4	0.151	901.4	1.10	4.35×10^3
200	1:37	18.8	4.4	0.151	910.2	0.97	3.82×10^3
200	1:35	19.4	4.2	0.166	900.9	0.93	3.67×10^3
300	1:27	14.1	4.0	0.166	801.3	1.13	4.43×10^3
300	1:21	16.2	4.3	0.166	815.7	1.01	3.95×10^3
300	1:16	18.3	4.0	0.166	788.6	0.86	3.37×10^3
300	1:22	19.4	3.8	0.160	844.6	0.87	3.75×10^3
400	1:11	14.1	3.5	0.151	801.6	1.14	4.44×10^3
400	1:10	16.4	3.5	0.151	841.9	1.03	4.01×10^3
400	1:10	18.2	4.4	0.151	801.3	0.88	3.44×10^3
400	1:21	19.1	4.7	0.169	828.8	0.87	3.51×10^3

same estimated hole volume per total irradiation fluence of about $3.54 \times 10^3 \mu\text{m}^3/\text{J}/\text{cm}^2$. Therefore, under various irradiation conditions, the hole depth and estimated hole volume per total irradiation fluence depended on the fluence per single pulse but did not depend on the energy ratio in the laser pulse waveform or repetition rate.

Conclusion

Short-pulse CO₂ laser drilling in crown glass with a large thermal expansion coefficient of $94 \times 10^{-7}/\text{K}$ was investigated. The short-pulse CO₂ laser had a spike pulse width of about 250 ns, a pulse tail length of 31.4 to 134.7 μs , an energy ratio of 1:7 to 1:92, and a fluence per single pulse of 6.0 to 37.9 J/cm^2 at a repetition rate of 1 to 400 Hz. The short-pulse CO₂ laser with a tunable pulse tail operating at a repetition rate of 150 to 400 Hz produced crack-free holes without using any kind of cooling system in the processing area. In contrast, cracks were produced at a repetition rate of 90 Hz or less. The hole depth and the estimated hole volume per total irradiation fluence depended on the fluence per single pulse but did not depend on the laser pulse waveform with an energy ratio of 1:10 to 1:45 and a repetition rate of 200 to 400 Hz. In our next experiment, we will investigate various glass drilling, cutting, and grooving processes by a short-pulse CO₂ laser with tunable laser pulse waveforms operating at a repetition rate of 500 Hz to 1 kHz.

Acknowledgments This work was supported by JST A-STEP, No. AS3015041S. We would like to thank Seidensha Electronics CO., LTD of Japan.

Funding This work was supported by JST A-STEP, grant No. AS3015041S.

Data Availability The data that support the findings of this study are available from the corresponding author upon reasonable request.

Declarations

Competing Interests The authors declare no competing interests.

References

1. Maini, A.: Lasers and Optoelectronics: Fundamentals, Devices and Applications. Wiley, Hoboken (2013)
2. Choi, H.K., et al.: Formation of cylindrical micro-lens array on fused silica glass surface using CO₂ laser assisted reshaping technique. *Opt. Laser Technol.* **75**, 63–70 (2015)
3. Liu, Y.Z.: Coaxial waterjet-assisted laser drilling of film cooling holes in turbine blades. *Int. J. Mach. Tools Manuf.* **150** (2020)
4. McNally, C.A., Folkles, J., Pashby, I.R.: Laser drilling of cooling holes in aeroengines: state of the art and future challenges. *Mater. Sci. Technol.* **20**, 805–813 (2004)
5. Hof, L.A., Ziki, J.A.: Micro-hole drilling on glass substrates—a review. *Micromachines.* **8**, 1–23 (2017)

6. Ogura, H., Yoshida, Y.: Hole drilling of glass substrates with a CO₂ laser. *Jpn. J. Appl. Phys.* **42**, 2881–2886 (2003)
7. Irawan, R., Swee Chuan, T., Chia Meng, T., Khay Ming, T.: Rapid constructions of microstructures for optical fiber sensors using a commercial CO₂ laser system. *Open Biomed. Eng. J.* **2**, 28–35 (2008)
8. Yang, M., Li, Y., Wang, D.N.: Long-period fiber gratings fabricated by use of defocused CO₂ laser beam for polarization-dependent loss enhancement. *J. Opt. Soc. Am. B.* **26**, 1203 (2009)
9. Oh, S., Lee, K.R., Paek, U.-C., Chung, Y.: Fabrication of helical long-period fiber gratings by use of a CO₂ laser. *Opt. Lett.* **29**, 1464 (2004)
10. Klank, H., Kutter, J.P., Geschke, O.: CO₂-laser micromachining and back-end processing for rapid production of PMMA-based microfluidic systems. *Lab Chip.* **2**, 242–246 (2002)
11. Cheng, J.Y., Wei, C.W., Hsu, K.H., Young, T.H.: Direct-write laser micromachining and universal surface modification of PMMA for device development. *Sensors Actuators B Chem.* **99**, 186–196 (2004)
12. Yeo, C.Y., Tam, S.C., Jana, S., Lau, M.W.S.: A technical review of the laser drilling of aerospace materials. *J. Mater. Process. Technol.* **42**, 15–49 (1994)
13. Uno, K., Yamamoto, T., Akitsu, T., Jitsuno, T.: Glass drilling by longitudinally excited CO₂ laser with short laser pulse. *Proc. SPIE.* **9350**, 93501E (2015)
14. Uno, K., Nakamura, K., Goto, T., Jitsuno, T.: Longitudinally excited CO₂ laser with short laser pulse like tea CO₂ laser. *J Infrared. Millimeter. Terahertz Waves.* **30**, 1123–1130 (2009)
15. Uno, K., Yamamoto, T., Watanabe, M., Akitsu, T., Jitsuno, T.: SiO₂ -glass drilling by short-pulse CO₂ laser with controllable pulse-tail energy. *Proc. SPIE.* **9735**, 973519 (2016)
16. Uno, K., Jitsuno, T.: Control of laser pulse waveform in longitudinally excited CO₂ laser by adjustment of excitation circuit. *Opt. Laser Technol.* **101**, 195–201 (2018)
17. Uno, K., Watarai, S., Kodama, Y., Yoneya, K., Jitsuno, T.: Longitudinally excited short-pulse CO₂ laser with large discharge tube without preionization. *Opt. Laser Technol.* **148**, 107745 (2022)
18. Rihakova, L., Chmelickova, H.: Laser micromachining of glass, silicon, and ceramics. *Adv. Mater. Sci. Eng.* **2015**, 1–6 (2015)
19. Schulz, W., Eppelt, U., Poprawe, R.: Review on laser drilling I. fundamentals, modeling, and simulation. *J. Laser Appl.* **25**, 012006 (2013)
20. Salleo, A., Sands, T., Génin, F.Y.: Machining of transparent materials using an IR and UV nanosecond pulsed laser. *Appl. Phys. A Mater. Sci. Process.* **71**, 601–608 (2000)
21. Zhang, C., et al.: Influence of pulse length on heat affected zones of evaporatively-mitigated damages of fused silica optics by CO₂ laser. *Opt. Lasers Eng.* **125** (2020)
22. Guignard, F., Autric, M.L., Baudinaud, V.: Temperature and residual stress evolution in CO₂-laser-irradiated glass. *High-Power Laser Ablation.* **3343**, 534–545 (1998)
23. Okazaki, K., et al.: Sub-wavelength micromachining of silica glass by irradiation of CO₂ laser with Fresnel diffraction. *Appl. Phys. A Mater. Sci. Process.* **104**, 593–599 (2011)
24. Nakamura, R., et al.: Cutting complex shape in glass substrate with pulsed CO₂ laser. *Rev. Laser Eng.* **43**, 28–30 (2015)
25. Dyer, P.E., Waldeck, I., Roberts, G.C.: Fine-hole drilling in Upilex polyimide and glass by TEA CO₂ laser ablation. *J. Phys. D. Appl. Phys.* **30**, 6 (1997)
26. Salonitis, K., Stournaras, A., Tsoukantas, G., Stavropoulos, P., Chryssolouris, G.: A theoretical and experimental investigation on limitations of pulsed laser drilling. *J. Mater. Process. Technol.* **183**, 96–103 (2007)
27. Förster, D.J., Weber, R., Holder, D., Graf, T.: Estimation of the depth limit for percussion drilling with picosecond laser pulses. *Opt. Express.* **26**, 11546 (2018)

Publisher's Note Springer Nature remains neutral with regard to jurisdictional claims in published maps and institutional affiliations.